Journal of Manufacturing Engineering, June, 2013, Vol. 8, Issue. 2, pp 117-122

EVALUATION OF MIG WELDING SURFACES USING GAUSSIAN DISTRIBUTION

***Senthil Kumar G[1] and Natarajan U[2]**

[1]Department of Mechanical Engineering, Velammal College of Engg & Tech. Madurai, Tamil Nadu, India
[2] Department of Mechnaical Engineering, A. C College of Engg & Tech., Karaikudi, Tamil Nadu, India

ABSTRACT

In this paper, an effort has been taken to assess the qualities of MIG (Metal Inert Gas) welded joints using vision system and the assumption that the vertical section of the surface of a weld image can be estimated by Gaussian distribution(normal curve). The surface variations of the weld image caused by defects are used to categorize welds as good weld, and no weld. This paper consists of two major divisions: weld extraction and surface quality evaluation. Initially weld beads are extracted from the MIG Welded joints through CCD camera of a machine vision system. The grey level values of the pixels from the captured images are assumed to fit a Gaussian distribution, and then determine their qualities. This method is tested with 80 images of good and no weld. Finally, it is concluded that this method may be used for extraction of features in vision inspection system of the quality of welded surfaces.

Key words: *MIG Welding, Welding Defects, Vision System and Gaussian Distribution*

1. Introduction

Inspection of welded joints in manufacturing industries is essential to ensure that the quality of weld meets the requirements of the design and operation, thus to assure safety and reliability. Gas metal arc welding (GMAW), sometimes referred to by its subtype namely metal inert gas (MIG) welding, is a semi-automatic or automatic arc welding process in which a continuous and consumable wire electrode and a shielding gas are fed through a welding gun. The trustworthy detection of weld defects is one of the most important tasks in non-destructive testing (NDT). Upgrading in these methods is necessary, because the human inspection of weld defects is a hard and difficult task when large numbers of welds are to be inspected. Assortments of studies that have been analyzed in open literature in these areas are reviewed. Visual inspection is the primary assessment method of many quality control programs. It can be carried out easily and inexpensively. It is used most effectively for the inspection of welds if quick detection and correction of flaws or process related problems resulting in significant cost savings [1]. H. I. Safeek et al [2] established a novel automated vision system to detect and assess the welding defects of gas pipelines using the radiographic films. S. Jagannathan [3] investigated an automatic inspection system of wave-soldered joints by using intelligent histogram regarding technique that divides the grey level histogram of the captured image from a joint into different modes. Tae-Hyeon [4] explained an efficient technique for solder joint inspection using three layers of ring-shaped LEDs with different illumination angles. T.Warren Liao [5] expanded a weld extraction methodology based on the observation that the intensity plot of a weld looks more like Gaussian than the other objects in the image. H.I.Safeek et al [6] introduced a novel automated vision system with AutoWDA (Automatic welding Defect Assessments) algorithm to detect and assess the welding defects of gas pipelines using the radiographic films. In his method, grey scale values of neighborhood pixels were used as boundary chain code algorithm to detect the welding defects. Joongho Chang et al [7] developed cork quality classification system using linear transformation as a function of the distance between the average and the grey level of each pixel within the windowed area. B.Ramamoorthy et al [8] estimated the surface roughness of machined surfaces using machine vision system.. Romeu R. da Silva et al [9] estimated the accuracy of classification of welding defects using geometric features of the pixel values.

Grey scale intensity value of pixels depends on the amount of light generated by the light sources, nature of the welded surface and the amount of light that is captured by the sensor (camera) [14-17]. In this work, front lighting system with CCD camera is used to capture the images of the MIG welded joints and grey values of pixels have been extracted from the images. These are used to study the closeness of the vertical

**Corresponding Author - E- mail: senthilgandhi@ymail.com*

cross section of the welded surface to Gaussian distribution as surmised by T.Warren Liao [5] and the fitness of the same is tested through chi-square test. In refine with the trend of this statistical approach, the values of intensity of the pixels are divided into a suitable number of class intervals (grouping) and record the observations of grey scale values. Finally, the observations of the images like good weld and no weld are fitted to the Gaussian distribution through calculated mean and standard deviations of the respective images and then expected normal frequencies are calculated and fitness is verified by using chi-square test. In general, the calibration process is difficult to carry out in industrial environment due to vibrations and random movements that vary with time [10]. Therefore, any calibration process is not followed in this method. This article is organized as follows: second section demonstrates the system overview followed by third section where carrying out tests in which preparation of weld joint and image capturing are explained. Then pre processing of the captured images of different types of weld described in fourth section. In the fifth section, fitness of Gaussian distribution and Chi-square test for the images has been elaborately discussed. In section six, the results are analyzed both graphically and analytically. Finally, section seven concludes about this work with further scope.

2. System Overview

Rapid-I machine vision system photograph is shown in Fig.1. which is used to capture the images welded surfaces. Vision based inspection systems are set of new technologies for non-contact inspections and measurements. The instruments integrate multitude of technologies including digital imaging, electronics, embedded systems and software. The Rapid-I, a vision based metrology instrument utilizes these innovative technologies to enable us to do precise inspections. It is capable of carrying out diverse measurement tasks including all basic 2D measurements, depth and even threads parameters. Its primary advantage lies in its high-resolution optics combined with precision work stage and power software. The quality of imaging cannot be changed, if the hardware is not suitably designed [14]. Host computer controls front lighting system and input camera. Full operations including image capturing and inspection software are executed in the host computer. This vision system is used to capture the images of the welded joints. The size of the image captured by the vision system is 800 x 600 pixels.

Fig. 1 RAPID I Computer vision system used to capture surface of MIG welding joints.

3. Experimentation

First of all different types of joints like acceptable and unacceptable joints (good and no weld) in the single V groove butt welding joint in MIG welding process have been prepared as per Standard EN 25817. Carbon steel plate size of 80 x 20 x 4 mm is used as a parent material in this work. The voltage and current maintained during welding are 27V and 260 Amps respectively. ER 70 S6 with 1.2 mm diameter electrode is used in this experiment. Carbon dioxide is supplied during the welding process and standoff distance is maintained at15mm.

Secondly, based on the values obtained for the various measurements acceptance or non acceptance of the weld will be decided in conformity with EN 25817 acceptance levels for intermediate service conditions. The different types of acceptable and unacceptable groove weld profile in butt joint are shown in Fig.2. Fig.2 (a) shows the image of good weld, h, b and t denote reinforcement height, width of the weld and thickness of the work piece respectively. The weld is accepted as good weld when the reinforcement height (h) lies in the range $h \leq 1mm+0.15b$, maximum $\leq 7mm$. Fig.2 (b) illustrates No weld. When the groove surface is not filled, then it is called No weld.

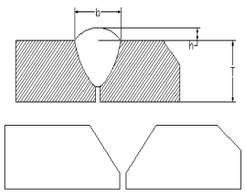

Fig. 2 a) Good weld b) No weld

Where, h = reinforcement in mm
b = width of the weld in mm
t = work piece thickness

Then the pieces of welded work are placed on the table under the camera of the vision system one by one with proper illumination to capture the required image. The types of welds, for which welding defects are inspected, include good weld, excess weld, insufficient weld and no weld. The LEDs of the system are turned on and the weld images are captured. The captured image for good weld is shown in Fig: 3.a and image of no weld is shown in Fig: 3.b.

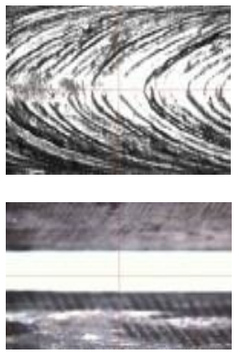

Fig.3 a) Image of Good weld b) Image of no weld

4. Pre Processing

Image processing seeks to modify and prepare the pixel values of a digitized image to produce more suitable form for subsequent operations. In this process, image is read and stored into an array for further processing. RGB images are then converted to greyscale images by eliminating the hue and saturation information by applying mean filtering for retaining the luminance.A region of interest of the image is cropped manually for further processing. Grey scale values of pixels of the cropped image of good weld are listed in Table: 1.

Table 1: Pixel Values for Good Weld

Column / Row	1	2	....	9	10
1	59	58	....	119	119
2	61	62	....	105	105
.	.	.	.	.	.
.	.	.	.	.	.
196	21	18	....	36	37
197	24	22	....	45	45
198	24	23	....	49	49

5. Fitness of Distribution

In probability theory, the Gaussian (or) normal distribution is a continuous probability distribution that is often used as a first approximation to describe real-valued random variables that tend to cluster around a single mean value. The graph of the associated probability density function given below is "bell"-shaped, and is known as the Gaussian function or bell curve [12]

$$f(x) = \begin{cases} \frac{1}{\sqrt{2\pi\sigma^2}} \; e^{-\frac{(x-\mu)^2}{2\sigma^2}} \\ -\infty \; < x < \infty \end{cases} \quad (1)$$

where parameter μ is the mean (location of the central tendency) and σ^2 is the variance (the measure of the deviation from the mean of the distribution). The distribution with $\mu = 0$ and $\sigma^2 = 1$ is called the standard normal distribution. This is also considered the most prominent probability distribution in statistics. There are several reasons for this: First, the normal distribution is very tractable analytically, that is, a large number of results involving this distribution can be derived in explicit form. Secondly, the normal distribution arises as the outcome of the central limit theorem, which states that under mild conditions the sum of a large number of random variables is distributed approximately normally. Finally, the "bell" shape of the probability curve of the normal distribution makes it a convenient choice for modeling a large variety of random variables encountered in practice. Chi-square test has a large number of applications in statistics. It is a powerful test for testing the significance of the discrepancy between theory and experiment.

Table 2: Percentage of pixel values are calculated and taken as frequency (f)

Class – interval	Mid value (x)	Average intensity value (i)	Percentage of intensity value $f_i = \left({}^{i}/_{\sum i}\right)100$	frequency f_i
1-18	9.5	1432.00	6.17	6
19-36	27.5	2092.00	9.01	9
37-54	45.5	2437.20	10.50	11
55-72	63.5	3313.00	14.28	14
73-90	81.5	2333.00	10.05	10
91-108	99.5	3494.00	15.06	15
109-126	117.5	2250.10	9.69	10
127-144	135.5	2085.80	8.99	9
145-162	153.5	1184.00	5.10	5
163-180	171.5	1655.80	7.13	7
181-198	189.5	921.00	3.97	4
	Total	23197.90	100	100

In this work, the column values are summarized and the mid values of the successive 18 values are taken and assumed as x. The grey scale pixel

values of all 18 rows, 11 columns are summarized, and its percentage of pixel values are calculated and taken as frequency (f) and tabulated in Table:2.

The arithmetic mean of a set of observations is the sum of the observed values divided by their number. The arithmetic mean of this distribution is calculated as follows

$$\mu = A + \frac{1}{N}\sum_{i=1}^{n} f_i d_i \qquad (2)$$

If the values of x and f are large, the calculation of mean is quite time consuming and tedious. The arithmetic computations are reduced to a great extent by taking the deviations of the given values from any arbitrary value 'A'. any number can serve the purpose of arbitrary value 'A' but, usually,

the value of x corresponding to the middle part of the distribution will be more convenient. In case of grouped frequency distribution, the computation is reduced largely by taking

$$d_i = \frac{x_i - A}{c} \qquad (3)$$

where A is an arbitrary value and C is the common magnitude of class interval.

The arithmetic mean of this distribution is $(\mu) = 91.22$ where $A = 81.5, C = 18$ & $N = 100$

Standard deviation (σ) is the positive square root of the arithmetic mean of the squares of the deviations of the given values from their arithmetic mean. It is also the best and most powerful measure of dispersion. In this case, variance is independent of change of origin but not of scale. The Standard deviation (σ) is calculated in this distribution as follows

$$\sigma = \sqrt{c^2\left\{\frac{1}{N}\sum_{i=1}^{n} f_i {d_i}^2 - \left(\frac{1}{N}\sum_{i=1}^{n} f_i d_i\right)^2\right\}} \qquad (4)$$

In order to fit a normal distribution to the given data, calculated values of mean (μ) and standard deviations (σ) from the given data are used in the equation of the normal curve and expected normal frequencies are calculated. To calculate the expected normal frequencies, first the standard normal variates corresponding to the mid-point of each of the class interval are computed by the following formula

$$Z = \frac{x_i - \mu}{\sigma} \qquad (5)$$

Then the ordinate values of normal curves Φ(z) are computed from the normal distribution tables. Finally, ordinates of normal probability curve values are multiplied by Nc / σ and the expected normal frequencies are obtained. Converting the expected frequencies as whole numbers such that total of expected frequencies is 100. χ^2-distribution is used to test the goodness of fit and also the independence of attributes. For the χ^2-test of goodness of fit to be effective and valid, number of observations must be large, individual frequencies must not be too small i.e. $O_i \geq 10$(incase <10 it is combined with the neighboring frequencies), number of classes must be neither too small nor too large [12-14]. In this experiment, it is assumed that random samples (grey scale of pixels) have been drawn from a normal population with a specific variance (σ^2). They are considered as observed frequencies (O_i) and are tabulated along with expected frequencies (E_i) in adjacent column in table.6. In order to test the goodness of fit, differences between observed and expected frequencies have been determined after combining the end classes to make the individual frequencies neither too small nor too large, they are tabulated in table.3.

Table 3: Observed and Expected Frequencies of Grouped Intervals of Good Weld.

Class	Observed frequency O_i	Expected frequency E_i
1	6	4
2	9	7
3	11	10
4	14	13
5	10	15
6	15	15
7	10	13
8	9	10
9	5	7
10	7	4
11	4	2

The number of degrees of freedom χ^2 is given by ν = Number of classes (n) – Number of statistical constants obtained from the data (k). In this experiment, to find the expected frequencies, the values of $\sum O_i$, μ and σ have been used. Hence Degrees of freedom ν = 8 –3 = 5. From the χ^2-table for the 5% level of significance (LOS), $\chi^2_{5\%}(\nu=5) = 11.09$.Since $\chi_o^2 < \chi^2_{5\%}$, the null hypothesis which assumes that the grey scale value based distribution is nearly normal, is accepted and normal fit for this distribution is satisfactory. Then the test of goodness of fit is applied to all types of samples of welded images one by one and analyzed. Samples of good weld images are accepted and images of no weld are not accepted at 5 % level of significance (LOS).

6. Results and Discussions

Comparison of observed frequencies and expected frequencies of grey scale values of pixels are shown in Fig.4-5.The ordinate decreases rapidly from the maximum as x increases numerically. The graph is concave downward at x = μ and it is concave upward for large numerical value of x. The points at which the concavity changes are called the points of inflexion of the curve. It is proved that the points of inflexion of the normal probability curve occur at x = $\mu \pm \sigma$, that is, at points which are at a distance of σ on either side of x = μ. Thus, if σ is relatively large; the curve tends to be peaked.

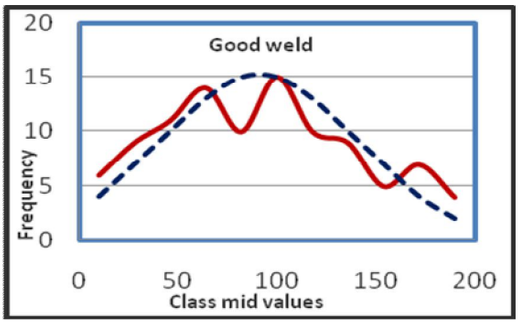

Fig. 4 Probability Curves of Observed and Expected Frequency of Good Weld

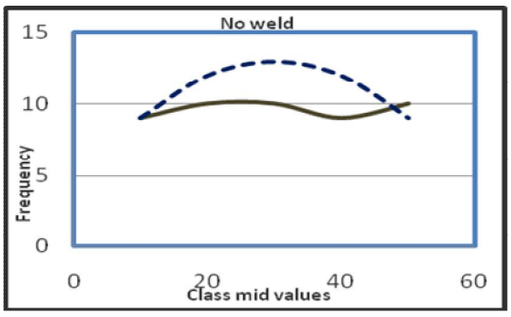

Fig. 5 Probability Curves of Observed and Expected Frequency of No Weld

In this experiment, the Gaussian and χ^2 test have been used to analyze the significance of goodness of fit in welded images. This method is applied for good and no weld images with 80 samples that contain 40 samples of each type. Values of means and standard deviations of all samples are listed in table.8. Fitness of normal distribution and validation of χ^2 tests of images are listed in table.9.A close read-through of the graphic

Table 4: Calculated and Critical value of Chi-square Distribution for Good Weld.

Sample No	Good weld				No weld			
	χ^2 Value	d of	χ^2 5% LOS	Accept Reject	χ^2 Value	d of	χ^2 5% LOS	Accept /Reject
1	5.43	5	11.09	Accept	14.01	4	9.488	Reject
2	6.06	4	9.488	Accept	15.03	5	11.09	Reject
3	5.95	4	9.488	Accept	15.03	5	11.09	Reject
4	9.47	4	9.488	Accept	15.03	5	11.09	Reject
5	4.83	4	9.488	Accept	15.03	5	11.09	Reject
6	5.22	4	9.488	Accept	15.03	5	11.09	Reject
7	6.50	4	9.488	Accept	15.03	5	11.09	Reject
8	4.16	4	9.488	Accept	14.01	4	9.488	Reject
9	5.15	4	9.488	Accept	15.03	5	11.09	Reject
1	3.37	4	9.488	Accept	15.03	5	11.09	Reject
1	3.91	4	9.488	Accept	15.03	5	11.09	Reject
1	4.98	4	9.488	Accept	15.03	5	11.09	Reject
1	5.80	4	9.488	Accept	15.03	5	11.09	Reject
1	5.33	4	9.488	Accept	15.03	5	11.09	Reject
1	3.26	4	9.488	Accept	14.01	4	9.488	Reject
1	3.37	4	9.488	Accept	15.03	5	11.09	Reject
1	4.80	3	7.815	Accept	15.03	5	11.09	Reject
1	2.55	4	9.488	Accept	15.03	5	11.09	Reject
1	4.26	3	7.815	Accept	15.03	5	11.09	Reject
2	1.36	4	9.488	Accept	15.03	5	11.09	Reject
2	3.35	4	9.488	Accept	15.03	5	11.09	Reject
2	1.12	4	9.488	Accept	15.03	5	11.09	Reject
2	7.46	4	9.488	Accept	15.03	5	11.09	Reject
2	3.28	4	9.488	Accept	15.03	5	11.09	Reject
2	11.99	5	11.09	Accept	15.03	5	11.09	Reject
2	3.02	5	11.09	Accept	15.03	5	11.09	Reject
2	3.36	4	9.488	Accept	15.03	5	11.09	Reject
2	3.39	4	9.488	Accept	15.03	5	11.09	Reject
2	2.50	3	7.815	Accept	15.03	5	11.09	Reject
3	4.20	5	11.09	Accept	15.03	5	11.09	Reject
3	1.68	4	9.488	Accept	14.01	4	9.488	Reject
3	3.07	4	9.488	Accept	15.03	5	11.09	Reject
3	3.74	3	7.815	Accept	15.03	5	11.09	Reject
3	0.97	3	7.815	Accept	15.03	5	11.09	Reject
3	2.30	4	9.488	Accept	15.03	5	11.09	Reject
3	1.59	3	7.815	Accept	15.03	5	11.09	Reject
3	1.88	4	9.488	Accept	15.03	5	11.09	Reject
3	0.86	4	9.488	Accept	15.03	5	11.09	Reject
3	9.24	3	7.815	Accept	15.03	5	11.09	Reject
4	3.73	4	9.488	Accept	15.03	5	11.09	Reject

representations of the observed and expected frequencies in respect of good and no welds exposes the following aspects.

1) Having in mind the assumption that all the samples have been drawn from normal populations, it is satisfactory to note that the graphs of expected frequencies of all images of good welds are more or less of the Gaussion type curves as they are bell shaped, concave downward near the central point and concave upward near the ends on either side of the central point.
2) The deviations of the graphs of observed frequencies from those of expected frequencies may be attributed to fluctuations of sampling and uncertainties associated with the process of welding and image processing.
3) However, the graphs of expected frequencies may be regarded as free hand smooth curves of the corresponding graphs of the observed frequencies.
4) The graph of the observed frequency curve corresponding to no welds is different from good weld. In particular, the graph corresponding no weld is flat near top, indicating that there is no welding material near the centre point.

7. Conclusion

The statistical technique used in this work to analyze the closeness to normality through Gaussian distribution and Chi-square test for images of MIG welded joints and no weld may be further utilized to extract the set of features that are used in vision inspection for welded joints. The properties of Gaussian distribution curves to be considered for the extraction of set of features like mean, median, mode and standard deviation. These properties of normal distribution curve are more informative than other grey scale value- related features. These test results show that this methodology is capable of exhibiting the features of welded images and may be used to determine their qualities. Thus, the set of features of grey scale values of welded images based on Gaussian (or) normal distribution curve will be exercised in further research that has been planned to develop the vision based inspection systems for MIG welded joints.

References

1. *Wang G and Liao T W (2002), "Automatic Identification of Different Types of Welding Defects in Radiographic Images", NDT&E International, Vol. 35, 519-528.*
2. *Shafeek H I, Adelmawla E S, Abdel-Shafy A A and Elewa I M (2004), "Automatic Inspection of Gas Pipeline Welding Defects using an Expert Vision System", NDT&E International, Vol. 37, 301-307.*
3. *Jagannathan S (1997), "Automatic Inspection of Wave Soldered Joints using Neural Networks", Journal of Manufacturing Systems, Vol. 16, 389-398.*
4. *Tae-Hyeon Kim, Tai-Hoon Cho, Young Shik Moon, and Sung Han Park (1999), "Visual Inpection System for the Classification of Solder Joints", Pattern Recognition, Vol. 32, 565-575.*
5. *Warren Liao T and Yueming Li (1998), "An Automated Radiographic NDT System Weld Inspection", NDT&E International, Vol. 31, 183-192.*
6. *Warren Liao T (2009), "Improving the Accuracy of Computer-Aided Radiographic Weld Inspection by Feature Selection", NDT&E International, Vol. 42, 229-239.*
7. *Joongho Chang et al (1997), "Cork Quality Classification System using a Unified Image Processing and Fuzzy- Neural Network Methodology", IEEE Transactions of Networks, Vol. 8, 964-974.*
8. *Jagannathan S (1992), "Intelligent Inspection of Wave Soldered Joints - Technical Report", Journal of Manufacturing Systems, Vol. 11, 137-143.*
9. *Romeu R and da Silva et al (2005), "Estimated Accuracy of Classification of Defects Detected in Welded Joints by Radiographic Tests", NDT&E International, Vol. 38, 335-343.*
10. *Gauss M, Buerkle A, Laengle T, Woern H, Stelter J, Ruhmkorf S and Middelmann R (2003), "Adaptive Robot Based Visual Inspection of Complex Parts", ISR.*
11. *Miguel Carrasco and Domingo Merry (2010), "Automatic Multiple View Inspection using Geometrical Tracking and Feature Analysis in Aluminum Wheels", Machine Vision and Applications.*
12. *Veerarajan T (2010), "Probability, Statistics and Random Processes", Third Edition, Tata McGraw-Hill Publishing.*
13. *Gupta S C and Kapoor V K (1999), "Fundamentals of Mathematical Statistics", Sultan Chand & Sons Publishing.*
14. *Sonka M, Hilavac H and Boyle R (1998), "Image Processing, Analysis and Machine Vision", Second Edition. PWS Publishing (USA).*
15. *Sonka M, Hilavac H and Boyle R (2011), "Digital Image Processing and Computer Vision", Fourth Edition. Cengage Learning Products.*
16. *Rafeal C Gonzalez and Richard E Woods (2002), "Digital Image, Second Edition Addison - Wesley.*
17. *Sridhar S (2011), "Digital Image Processing", First Edition, Oxford University Press.*

